Vibronic Coupling in Naphthalene Anion: Vibronic Coupling Density Analysis for Totally Symmetric Vibrational Modes

Tohru Sato,*,†,‡ Ken Tokunaga,‡,§ and Kazuyoshi Tanaka‡,#

Fukui Institute for Fundamental Chemistry, Kyoto University, Takano-Nishihiraki-cho 34-4, Sakyo-ku, Kyoto 606-8103, Japan, Department of Molecular Engineering, Graduate School of Engineering, Kyoto University, Nishikyo-ku, Kyoto 615-8510, Japan, and Core Research for Evolutional Science and Technology, Japan Science and Technology Agency (JST-CREST)

Received: August 30, 2007; In Final Form: October 25, 2007

Vibronic coupling, or electron−phonon coupling, of naphthalene is calculated. A method of vibronic coupling density analysis, which has been proposed for the vibronic coupling of the Jahn−Teller active modes in a Jahn−Teller molecule, is extended for totally symmetric vibrational modes of a molecule including a non-Jahn−Teller molecule. Contrary to non-totally-symmetric modes, orbital relaxation upon a charge transfer plays a crucial role in the vibronic coupling calculation for the totally symmetric modes. The method is applied for the ground state of the naphthalene anion to compare with that of the benzene anion. The relationship between the vibronic coupling density and a nuclear Fukui function is also discussed.

1. Introduction

Vibronic coupling is one of the fundamental interactions both in molecules and in extended systems.[1] The coupling is clearly observed in Jahn−Teller systems.[2,3] Strength of the coupling for a certain vibrational mode is measured by a vibronic coupling constant.

Recently, we have calculated the vibronic coupling for some Jahn−Teller molecules within a spectroscopic accuracy, and we have proposed a concept of *vibronic coupling density*, which provides a local picture of the coupling in a molecule.[4,5] For the vibronic coupling of a Jahn−Teller active mode, it is not the doubly occupied orbitals but the open level that can contribute to the coupling because of some symmetry reason. On the other hand, for totally symmetric modes either in the Jahn−Teller molecules or in the non-Jahn−Teller molecules, all the occupied orbitals can contribute to the coupling as long as the symmetry is permitted.[4,5]

In this article, we extend a method of the vibronic coupling density analysis for the totally symmetric modes and apply it to the ground state of the naphthalene anion to compare with that published for the benzene anion.[5]

Naphthalene is the second member of oligoacenes, and much research on the vibronic coupling has been done using both experimental and theoretical methods. Absorption, fluorescence, and photoelectron spectroscopy are important techniques in the observation of the vibronic coupling in the neutral[6−18] and the cationic state.[15,18−26] Simulated spectra have shown good agreements with these experimental data.[17,25,26] On the other hand, the vibronic coupling on the anionic state has not been observed with enough resolution because naphthalene has a negative electron affinity and is therefore unstable in the anionic state.[27−29] Previous theoretical studies on the vibronic coupling of naphthalene anion have concerned the superconducting transition temperature[30,31] or the intramolecular reorganization energy.[32]

The vibronic coupling is important also in chemical reaction theory. Cohen et al. have proposed a nuclear Fukui function based on the density functional theory.[33] The nuclear Fukui function has a close relation to the vibronic coupling density.

This article is organized as follows. In section 2, we define a vibronic Hamiltonian and introduce some notations which are used in the later sections. The vibronic coupling density is defined in section 3. Computational details are described in section 4. The calculated results are discussed in section 5. Finally, we summarize this work in section 7.

2. Vibronic Hamiltonian

We consider the structural change of a molecule upon a change of the electronic state, R → S, such as an electron addition, an electron removal (an ionization), or an electronic excitation. A reference nuclear configuration $\mathbf{R}_0$ is defined as a certain nuclear configuration of the molecule. In the case of a Jahn−Teller molecule, $\mathbf{R}_0$ is defined as a Jahn−Teller center[2] where the electronic state is degenerate, whereas, for a non-Jahn−Teller molecule, naphthalene in the present study, the optimized geometry of the ground state of the neutral state is taken as the reference nuclear configuration. We simply call the system consisting of the reference configuration $\mathbf{R}_0$ and electronic state a reference system R herein.

The change of the electronic state from R to S, R → S, will give rise to a deformation of the nuclear configuration, $\mathbf{R}_0 \rightarrow \mathbf{R}$. An arbitrary deformed structure with the electronic state S is called a system S hereafter. The molecular Hamiltonian for a deformed molecule with a nuclear configuration $\mathbf{R}$ can be written as

$$\mathscr{H}(\mathbf{r},\mathbf{R}) = \mathscr{T}_n(\mathbf{R}) + \mathscr{T}_e(\mathbf{r}) + \mathscr{U}(\mathbf{r},\mathbf{R}_0) + \sum_i \mathscr{V}_i Q_i + \frac{1}{2}\sum_i \sum_j \mathscr{W}_{ij} Q_i Q_j \quad (1)$$

* Corresponding author. E-mail: tsato@scl.kyoto-u.ac.jp.
† Fukui Institute for Fundamental Chemistry, Kyoto University.
‡ Department of Molecular Engineering, Graduate School of Engineering, Kyoto University.
§ Present address: Research and Development Center for Higher Education, Kyushu University, Ropponmatsu, Fukuoka 810-8560, Japan.
# JST-CREST.

10.1021/jp076962a CCC: $40.75
Published on Web 01/09/2008

where

$$\mathcal{V}_i = \left(\frac{\partial \mathcal{U}}{\partial Q_i}\right)_{\mathbf{R}_0} \qquad \mathcal{W}_{ij} = \left(\frac{\partial^2 \mathcal{U}}{\partial Q_i \partial Q_j}\right)_{\mathbf{R}_0} \tag{2}$$

$$\mathcal{U}(\mathbf{r},\mathbf{R}) = \mathcal{U}_{ee}(\mathbf{r}) + \mathcal{U}_{en}(\mathbf{r},\mathbf{R}) + \mathcal{U}_{nn}(\mathbf{R}) \tag{3}$$

$\mathcal{T}_n(\mathbf{R})$ is a nuclear kinetic energy operator, $\mathcal{T}_e(\mathbf{r})$ is an electronic kinetic energy operator, $\mathcal{U}_{ee}(\mathbf{r})$ is an electronic−electronic, $\mathcal{U}_{en}(\mathbf{r},\mathbf{R})$ is an electronic−nuclear, and $\mathcal{U}_{nn}(\mathbf{R})$ a nuclear−nuclear potential operators. $\mathcal{V}_i$ is called the electronic part of a linear vibronic operator. $\mathcal{W}_{ij}$ is called the electronic part of a quadratic vibronic operator. The electronic Hamiltonian is $\mathcal{H}_e = \mathcal{T}_e + \mathcal{U}_{ee} + \mathcal{U}_{en}$.

A vibronic wave function can be expanded in terms of the eigenfunctions $\Phi(\mathbf{r},\mathbf{R}_0)$ of the electronic Hamiltonian $\mathcal{H}_e(\mathbf{r},\mathbf{R}_0)$, which are called the crude adiabatic (CA) basis. We concentrate on the case that the electronic ground state n is nondegenerate. We obtain the vibronic Hamiltonian as

$$\mathcal{H} = \sum_i (\mathbf{T}(Q_i))_{nn} + \mathbf{E}(\mathbf{R}_0)_{nn} + \sum_i (\mathbf{V}_i)_{nn} Q_i + \frac{1}{2}\sum_i \sum_j (\mathbf{W}_{ij})_{nn} Q_i Q_j \tag{4}$$

where the second term is an eigenvalue of $\mathcal{H}_e(\mathbf{r},\mathbf{R}_0)$. Assuming that the last term, which contains the cross terms of the normal modes, Q_iQ_j, is vanishing in the system S,[34] the vibronic Hamiltonian is finally obtained as

$$\mathcal{H} = \sum_i -\frac{\hbar^2}{2}\left(\frac{\partial^2}{\partial Q_i^2}\right) + E_0 + \sum_i V_i Q_i + \sum_i \frac{1}{2}\omega_i^2 Q_i^2 \tag{5}$$

where ω_i is the frequency of a vibrational mode i of the reference system and

$$V_i = (\mathbf{V}_i)_{nn} = \langle \Phi_n(\mathbf{r},\mathbf{R}_0) | \mathcal{V}_i | \Phi_n(\mathbf{r},\mathbf{R}_0) \rangle \tag{6}$$

The quantity V_i is called a linear vibronic coupling constant.

3. Vibronic Coupling Density

We restrict ourselves to the case of an electron addition to an N-electron system. We define the N-electron state of the molecule and the equilibrium structure $\mathbf{R}_0$ as the reference system R.

Within the Born−Oppenheimer (BO) approximation, we can write the energy of the N-electron system as a function of the nuclear configuration $\mathbf{R}$:

$$E_N(\mathbf{R}) = \langle \Psi_N | \mathcal{T}_e | \Psi_N \rangle + \langle \Psi_N | \mathcal{U}_{en} | \Psi_N \rangle + \langle \Psi_N | \mathcal{U}_{ee} | \Psi_N \rangle + \mathcal{U}_{nn}(\mathbf{R}) \tag{7}$$

where Ψ_N is an electronic wave function of the N-electron state at $\mathbf{R}$. At the equilibrium configuration $\mathbf{R}_0$,

$$\left(\frac{\partial E_N}{\partial Q_i}\right)_{\mathbf{R}_0} = \left[\frac{\partial \langle \Psi_N | \mathcal{H}_e | \Psi_N \rangle}{\partial Q_i}\right]_{\mathbf{R}_0} + \left(\frac{\partial \mathcal{U}_{nn}}{\partial Q_i}\right)_{\mathbf{R}_0} = 0 \tag{8}$$

for an arbitrary mode i. This is the condition for the equilibrium nuclear configuration $\mathbf{R}_0$ of the reference system.

When an electron is added to the reference system R, the energy of the electronic state of the $(N+1)$-electron state is written as a function of the nuclear configuration $\mathbf{R}$,

$$E_{N+1}(\mathbf{R}) = \langle \Psi_{N+1} | \mathcal{T}_e | \Psi_{N+1} \rangle + \langle \Psi_{N+1} | \mathcal{U}_{en} | \Psi_{N+1} \rangle + \langle \Psi_{N+1} | \mathcal{U}_{ee} | \Psi_{N+1} \rangle + \mathcal{U}_{nn}(\mathbf{R}) \tag{9}$$

where Ψ_{N+1} is the electronic wave function of the $(N+1)$-electron system, which is regarded as the system S defined in the previous section. Now that the equilibrium configuration of the reference system is not stable in the $(N+1)$-electron system,

$$\left(\frac{\partial E_{N+1}}{\partial Q_i}\right)_{\mathbf{R}_0} = \left[\frac{\partial \langle \Psi_{N+1} | \mathcal{H}_e | \Psi_{N+1} \rangle}{\partial Q_i}\right]_{\mathbf{R}_0} + \left(\frac{\partial \mathcal{U}_{nn}}{\partial Q_i}\right)_{\mathbf{R}_0} \tag{10}$$

can have a finite value.

If the Hellmann−Feynman theorem can be applied to eq 10, though this is not always the case as we discuss later, we can obtain an equation for the vibronic coupling constant V_i of the $(N+1)$-electron system as

$$\left(\frac{\partial E_{N+1}}{\partial Q_i}\right)_{\mathbf{R}_0} = \langle \Psi_{N+1}(\mathbf{r},\mathbf{R}_0) | \mathcal{V}_i | \Psi_{N+1}(\mathbf{r},\mathbf{R}_0) \rangle = V_i \tag{11}$$

Therefore, V_i can be evaluated from the gradient of the BO potential with respect to the normal coordinate. However, we calculate V_i from the integral in eq 11, because we are interested in a local property of the vibronic coupling.

Except for a totally symmetric mode, the derivative of the nuclear−nuclear repulsion potential is vanishing because of the symmetry:

$$\left(\frac{\partial \mathcal{U}_{nn}}{\partial Q_i}\right)_{\mathbf{R}_0} = 0 \tag{12}$$

It is not necessary to consider the nuclear−nuclear repulsion term for such a mode. As for a totally symmetric mode, on the other hand, the nuclear−nuclear repulsion term plays an important role in the vibronic coupling calculation.

From the equilibrium condition for the reference system (8), the nuclear−nuclear repulsion term becomes

$$\left(\frac{\partial \mathcal{U}_{nn}}{\partial Q_i}\right)_{\mathbf{R}_0} = -\left(\frac{\partial \langle \Psi_N | \mathcal{H}_e | \Psi_N \rangle}{\partial Q_i}\right)_{\mathbf{R}_0} \tag{13}$$

This relation is a particular case of Feynman's electrostatic theorem.[35] Substituting eq 8 into eq 10, we obtain

$$\begin{aligned} V_i &= \left[\frac{\partial \langle \Psi_{N+1} | \mathcal{H}_e | \Psi_{N+1} \rangle}{\partial Q_i}\right]_{\mathbf{R}_0} - \left[\frac{\partial \langle \Psi_N | \mathcal{H}_e | \Psi_N \rangle}{\partial Q_i}\right]_{\mathbf{R}_0} \\ &= \int \rho_1(\mathbf{x})\, v_i(\mathbf{x})\, \mathrm{d}\tau - \int \rho_0(\mathbf{x})\, v_i(\mathbf{x})\, \mathrm{d}\tau \\ &= \int \Delta\rho(\mathbf{x})\, v_i(\mathbf{x})\, \mathrm{d}\tau = \int \eta_i(\mathbf{x}) d\tau \end{aligned} \tag{14}$$

where ρ_0 and ρ_1 are electron densities of the N- and $(N+1)$-electron systems, respectively, and $\Delta\rho(\mathbf{x}) = \rho_1(\mathbf{x}) - \rho_0(\mathbf{x})$ is the electron density difference. Furthermore v_i is a one-electron operator, the derivative of the electronic-nuclear potential operator, which yields

$$\left(\frac{\partial \mathcal{U}_{en}}{\partial Q_i}\right)_{\mathbf{R}_0} = \sum_{\nu}^{N \text{ or } N+1} v_i(\mathbf{x}_\nu) \tag{15}$$

after summation over N or $N+1$ electrons, and $\eta_i(\mathbf{x})$ is the vibronic coupling density

$$\eta_i(\mathbf{x}) = \Delta\rho(\mathbf{x})\, v_i(\mathbf{x}) \tag{16}$$

For a Jahn−Teller molecule within the Hartree−Fock approximation, we can write η_i for a Jahn−Teller active mode as

$$\eta_i(\mathbf{x}) = \rho_1(\mathbf{x})\, v_i(\mathbf{x}) = \rho_{\mathrm{SOMO}}(\mathbf{x})\, v_i(\mathbf{x}) \tag{17}$$

where SOMO means a singly occupied molecular orbital, because the doubly occupied orbitals do not contribute to the vibronic coupling constant because of the symmetry of Clebsch−Gordan coefficients.[4] From eq 16, it is found that V_i can be calculated as the integral of η_i over the space. The vibronic coupling density can significantly contribute to the vibronic coupling constant in the region where both $\Delta\rho(\mathbf{x})$ and $v_i(\mathbf{x})$ are large. Furthermore, $\eta_i(\mathbf{x})$ gives a local picture of the vibronic coupling of a molecule.

The vibronic coupling constant for $(N-1)$-electron systems and electronic excited states can be calculated from the electron density difference and potential derivative in the same way.

However, the Hellmann−Feynman theorem is not valid for a conventional LCAO wave function, as long as the center of the basis functions are not variationally optimized. To make the theorem applicable, some improvements have been proposed: (1) using floating basis, (2) optimizing the center of the basis function variationally, and (3) including the derivatives of the basis set. In the present calculation, we employed a basis set including the first derivatives.[36] As we discuss later, the Hellmann−Feynman theorem is approximately satisfied, when the basis set with their first derivatives is used. It is expected that the higher derivatives are included to the basis set, the more the validity of the Hellmann−Feynman theorem would increase.

4. Method of Calculations

We adopted naphthalene anion as a target molecule. The reference system R is the ground state of neutral naphthalene. The equilibrium structure of the reference system $\mathbf{R}_0$, vibrational structure, and electron density ρ_0 were calculated using the restricted Hartree−Fock (RHF) method. Figure 1 shows the vibrational modes.

To evaluate the electron density ρ_1, the electronic structure of naphthalene anion was calculated using the restricted open-shell Hartree−Fock (ROHF) method at the equilibrium structure of the reference system $\mathbf{R}_0$. We call ρ_1 *relaxed density* ρ_R hereafter. For comparison with ρ_R, we also calculated the electron density using frozen orbital approximation, or Koopmans' approximation, ρ_F:

$$\rho_F = \rho_0 + \rho_{\mathrm{LUMO}} \tag{18}$$

where ρ_{LUMO} is frontier electron density of LUMO of the reference N-electron system calculated with the RHF method. We call ρ_F *frozen density*.

We optimized the geometry $\mathbf{R}$ of the anion and estimated the stabilization energy ΔE_{BO} from $\mathbf{R}_0$ to $\mathbf{R}$, which corresponds to the reorganization energy within the BO approximation. On the other hand, the Hamiltonian (5) in the CA approximation can be rewritten as

$$E(\mathbf{R}) = E_0 + \sum_i \left\{ V_i Q_i + \frac{1}{2}\omega_i^2 Q_i^2 \right\} = E_0 + \sum_i \left\{ \frac{1}{2}\omega_i^2 \left(Q_i - \frac{V_i}{\omega_i^2} \right)^2 - \frac{V_i^2}{2\omega_i^2} \right\} \tag{19}$$

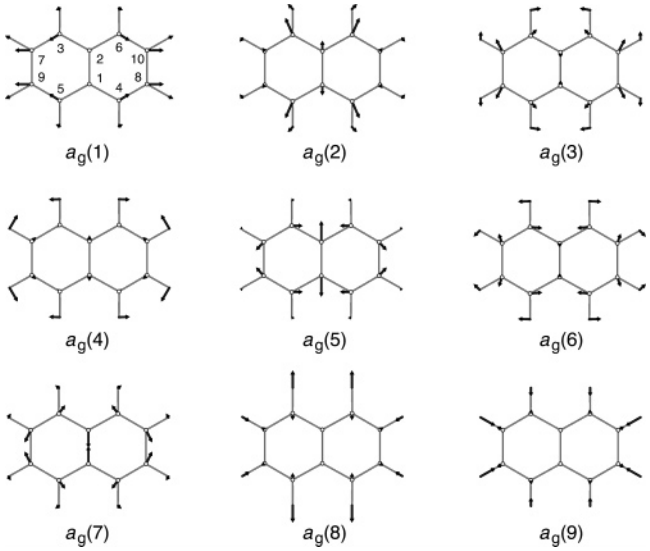

Figure 1. Vibrational modes of the reference system.

Therefore, the reorganization energy in the CA approximation can be expressed as

$$\Delta E_{\mathrm{CA}} = \sum_i \frac{V_i^2}{2\omega_i^2} \tag{20}$$

Throughout the article, the reorganization energy is given in electronvolts, wave number in cm^{-1}, and the other quantities are in atomic unit.

The basis set employed in all the calculations is the 6-31G basis set with the first derivatives. The calculations were performed using GAMESS program.[37]

5. Results and Discussion

5.1. Vibronic Coupling Constant. First, we confirmed the applicability of the Hellmann−Feynman theorem to the present model. Table 1 summarizes the frequencies and the deviation from the theorem for the reference system. Scaled values of frequency agree well with the experimental values.[38] The deviations from the Hellmann−Feynman theorem are large in the modes over 3000 cm^{-1}. Because these modes are localized on the C−H bonds as shown in Figure 1 and have high frequencies, the effect on the stabilization energy ΔE_{CA} is rather small (0.001 eV). Therefore, we can conclude that the Hellmann−Feynman theorem can be applied to the present model.

The calculated vibronic coupling constants are tabulated in Table 2. The calculation using the frozen density ρ_F by no means reproduces those calculated from the relaxed density ρ_R. In this respect, vibronic couplings for totally symmetric modes are quite different from those for Jahn−Teller active modes in which calculations assuming the Koopmans' approximation yields qualitatively satisfactory results. In the modes $a_g(2)$, $a_g(6)$, $a_g(8)$, and $a_g(9)$, the calculations using ρ_F and ρ_R result in different orders of magnitude with opposite signs, in $a_g(3)$ and $a_g(7)$ the couplings have different orders of magnitude, and in $a_g(1)$ they have opposite signs. Because the discrepancy is large in the low-frequency region, it greatly affects the reorganization energy. The frozen density ρ_F yields poor a result $\Delta E_{\mathrm{CA}} = 5.614$ eV. This is because the large values of V_i in the low-frequency region cause the overestimation of ΔE_{CA}. On the other hand, the reorganization energy using the relaxed density ρ_R in the CA approximation $\Delta E_{\mathrm{CA}} = 0.242$ eV is almost the same as the

TABLE 1: Calculated Values of Frequency (cm^{-1}), $\langle \Phi_N | \mathcal{V}_i | \Phi_N \rangle = V_i$ (10^{-4} au), and ΔE (eV) of a_g Modes[a]

		$a_g(1)$	$a_g(2)$	$a_g(3)$	$a_g(4)$	$a_g(5)$	$a_g(6)$	$a_g(7)$	$a_g(8)$	$a_g(9)$	ΔE
frequency	calc[b]	496	745	998	1154	1331	1454	1592	2997	3022	
	expt[c]	513	765	1020		1383	1464	1576		3057	
V_i		−0.06	−0.19	−0.16	−0.02	0.02	−0.04	−0.04	−0.28	0.83	0.001 (ΔE_{CA})

[a] ΔE_{CA} was calculated from V_i and unscaled ω_i. There is a good agreement between the theoretical and the experimental values of ω_i. Differences between V_i and $(\partial E_N/\partial Q_i)_{\mathbf{R}_0} = 0$ are small for the C−C stretching modes $a_g(5)-a_g(7)$, which yield large vibronic coupling constants, and that between ΔE_{CA} and $\Delta E_{BO} = 0$ is also small. Therefore, we can employ the Hellmann−Feynman theorem in the present calculations. [b] Scaled by 0.8992, the value for HF/6-31G(d,p).[42] [c] Raman scattering for single crystal of naphthalene.[38]

TABLE 2: Calculated Vibronic Coupling Constant V_i (10^{-4} au), Energy Gradient $(\partial E_{N+1}/\partial Q_i)_{\mathbf{R}_0}$ (10^{-4} au), and the Reorganization Energy ΔE (eV)[a]

		$a_g(1)$	$a_g(2)$	$a_g(3)$	$a_g(4)$	$a_g(5)$	$a_g(6)$	$a_g(7)$	$a_g(8)$	$a_g(9)$	ΔE
V_i	ρ_F	9.68	15.55	13.84	2.34	−5.22	4.70	−0.35	7.09	−12.15	5.614 (ΔE_{CA})
	ρ_R	−1.10	−0.61	0.64	2.11	−7.03	−0.17	−4.52	−0.21	1.84	0.242 (ΔE_{CA})
$(\partial E_{N+1}/\partial Q_i)_{\mathbf{R}_0}$		−1.04	−0.47	0.84	2.12	−7.06	−0.17	−4.47	0.07	0.98	0.239 (ΔE_{BO})
ref 31[b]		1.0	0.5		1.2	4.1		4.0			0.127
$\int \rho_{LUMO} v_i \, d\tau$		12.33	17.03	15.06	1.37	−6.76	5.37	0.02	9.26	−13.29	8.570 (ΔE_{CA})
$(\partial E_{N+1}/\partial Q_i)_{\mathbf{R}_0}^{B3LYP}$		−1.06	−0.61	−0.03	1.20	−4.11	−0.25	−3.97	−0.03	1.24	0.131 (ΔE_{BO})

[a] ΔE_{CA} in the CA approximation was calculated from V_i and unscaled ω_i. ΔE_{BO} was estimated from $E_{N+1}(\boldsymbol{R}_0) - E_{N+1}(\boldsymbol{R})$ in the BO approximation. Results of Kato and Yamabe are also tabulated for comparison. We also calculated the orbital vibronic coupling constant $\int \rho_{LUMO} v_i \, d\tau$ and energy gradient $(\partial E_{N+1}/\partial Q_i)_{\mathbf{R}_0}^{B3LYP}$ at the same level of theory, B3LYP/6-31G(d), as in ref 31. The reported values in ref 31 seem to be the energy gradient, though they have insisted they calculated the orbital vibronic coupling constant. [b] Absolute values of V_i calculated from the relation $V_i = \omega_i \sqrt{l_i}$, where l is the electron−phonon coupling constant defined in ref 31.

result in the BO approximation $\Delta E_{BO} = 0.239$ eV. It should be noted that ΔE_{CA} can be obtained from the calculation at the single point $\mathbf{R}_0$ without a geometry optimization of the anion.

Kato and Yamabe have reported the vibronic coupling constant of naphthalene anion.[31] Their results are also tabulated in Table 2. They have insisted that they calculated an orbital vibronic coupling constant, which is $\int \rho_{LUMO} v_i \, d\tau$ in the present notation. Therefore, it should approximately correspond to our results calculated using the frozen density. However, their results agree fairly well with the present values calculated using the relaxed density difference. To clarify this incomprehensible point, we calculated the orbital vibronic coupling constant $\int \rho_{LUMO} v_i \, d\tau$ and the energy gradient $(\partial E_{N+1}/\partial Q_i)_{\mathbf{R}_0}^{B3LYP}$ at the same level of theory, B3LYP/6-31G(d), as in ref 31 using Gaussian 03.[39] One can see from the table that the reported values in ref 31 seem to be not the orbital vibronic coupling constant but the energy gradient. The orbital vibronic coupling constant using ρ_{LUMO} is equal to the vibronic coupling constant using $\rho_F = \rho_0 + \rho_{LUMO}$ as long as the Hellmann−Feynman theorem is satisfied, because the contribution of ρ_0 is equivalent for the contribution of $\mathcal{V}_{nn}$. If one calculated a vibronic coupling constant following exactly the same procedure described in ref 31, one would obtain an unsatisfactory result, as we obtained in the sixth line of Table 2. In the present calculation using ρ_R, because the Hellmann−Feynman theorem is approximately valid by including the first derivatives of the basis functions, and the orbital relaxation is included, V_i is almost equal to the energy gradient as tabulated in the third and fourth lines of Table 2. It should be noted that the orbital relaxation is particularly important in non-Jahn−Teller molecules, because the orbital vibronic couplings of all the occupied orbitals contribute to the vibronic coupling constant.

5.2. Vibronic Coupling Density Analysis. Figure 2 shows the electron density differences using the frozen density ρ_F and the relaxed density ρ_R.

5.2.1. Frozen Electron Density. Because the electron density difference of ρ_F is equal to the frontier electron density of LUMO of naphthalene ρ_{LUMO}, ρ_F is positive everywhere, as shown in Figure 2a. Reflecting the orbital pattern of the LUMO, ρ_F is distributed greatly on C4 and C6. Because a nodal plane exists on the line connecting C1 and C2, the density on C1 and C2 is exactly zero. The density difference on C8 and C10 is small. It should be noted that the density difference distributes out of the molecular plane.

5.2.2. Relaxed Electron Density. Figure 2b shows the electron density difference using the relaxed density. The distribution of the density difference is rather complicated. The positive region with π character mainly comes from the LUMO. The positive region on C8 and C10 is increased after the relaxation. Moreover, it should be noted that there appear regions in which the electron density decreases upon the electron addition. Such negative regions are classified into two cases: the in-plane negative regions on C4, C6, C8, and C10 and the out-of-plane negative regions on C1 and C2. These negative regions originate from polarization that the orbitals of naphthalene anion are relaxed from those of the neutral molecule due to the additional electron density ρ_{LUMO}.

Different from a Jahn−Teller problem, the polarizations of the occupied orbitals play an important role in the vibronic coupling calculation in a non-Jahn−Teller molecule, because all the orbital vibronic couplings contribute to the vibronic coupling constant.

5.2.3. Derivative of Potential with Respect to Normal Coordinate. Figure 3 shows isosurfaces of the derivatives of the nuclear-electronic potential with respect to the normal coordinates. It is found that large contributions are located in the regions where the atoms move along bonds. As we will discuss later in detail, symmetric distribution of the derivative around a carbon atom gives rise to cancellation of the vibronic coupling density around the atom.

The $a_g(1)$ vibrational mode corresponds to one of $e_{2g}(1)$ modes of benzene. Note that the derivative $v_{a_g(1)}$ around C6 is asymmetric, and the electron density ρ_F has a symmetric distribution around C6. As for the benzene anion, no electron density is located here. On the other hand, the large density difference exists on C6 of naphthalene anion. Correspondingly the asymmetric distribution of $v_{a_g(1)}$ may give a large contribution to the vibronic coupling in naphthalene anion.

In addition, it should be noted that $v_{a_g(2)}$ exhibits asymmetric distributions around C2 and C6.

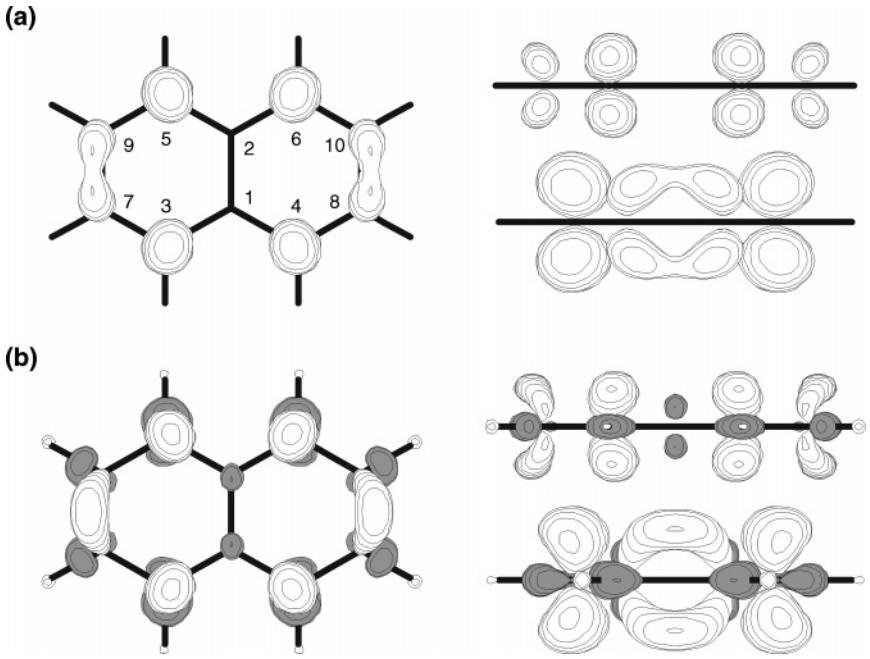

Figure 2. Electron density difference using (a) the frozen electron density ρ_F and (b) the relaxed electron density ρ_R. The white region is positive, and the gray region negative.

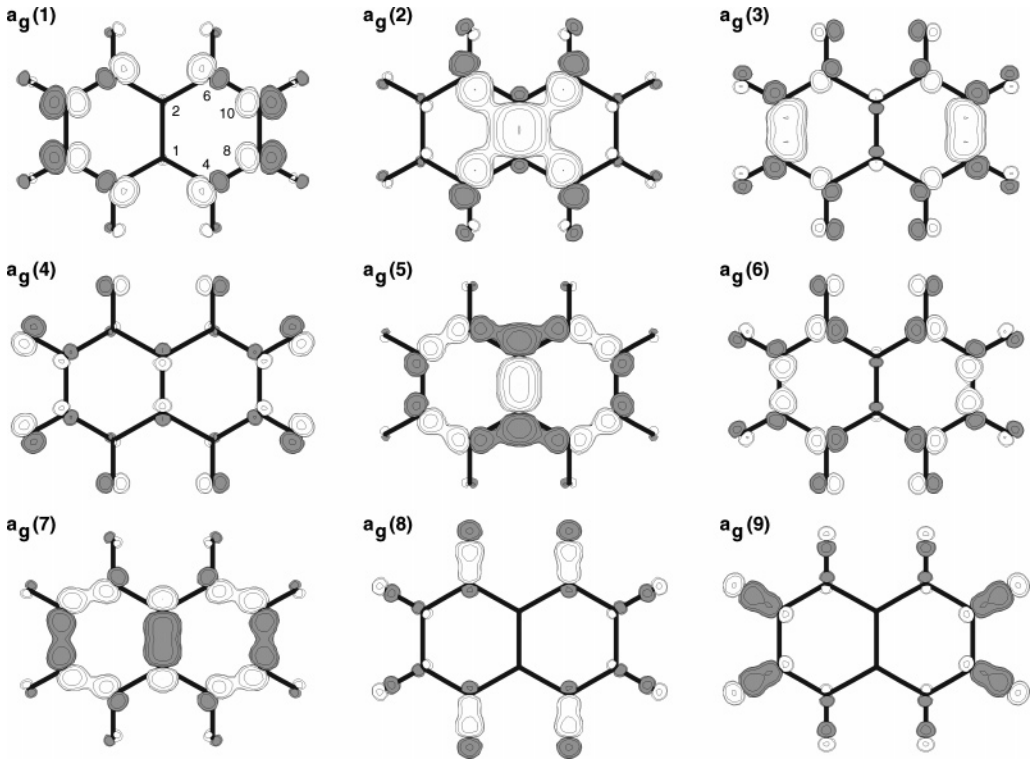

Figure 3. Derivative v_i of the nuclear-electronic potential $\mathcal{V}_{en}$ with respect to a normal coordinate Q_i. The white region is positive, and the gray region negative. The threshold of the isosurface is 0.01 atomic unit.

5.2.4. Frozen Vibronic Coupling Density. Figures 4 and 5 show the vibronic coupling density of naphthalene anion using the frozen density ρ_F. These distributions can be easily understood from Figures 2a and 3. Because $\rho_F \geq 0$, negative $\eta < 0$ is ascribed to negative $v < 0$. Furthermore, significantly asymmetric v yields large contribution to the vibronic coupling, because the ρ_F near an atom is almost symmetric.

We discuss $a_g(1)$, $a_g(2)$, $a_g(3)$, and $a_g(9)$ modes. In both $a_g(1)$ and $a_g(2)$ modes, ρ and v are greatly located near C6. In addition, because the anisotropy of the vibronic coupling density around C6 is large, the large net contribution to the vibronic coupling remains after cancellation.

Both ρ and v for $a_g(3)$ mode are large on the bond C8−C10. Thus $\eta_{a_g(3)}$ has large positive density on the bond. In other words, the reason why $V_{a_g(3)}$ is large is that the displacement of the mode is along the bond in which the frontier orbital has bonding character. The same situation occurs in cyclopentadienyl radical[4] and benzene radicals.[5]

Modes $a_g(8)$ and $a_g(9)$ are C−H stretching modes. Because v is anisotropic around the C atoms connecting to the H atoms,

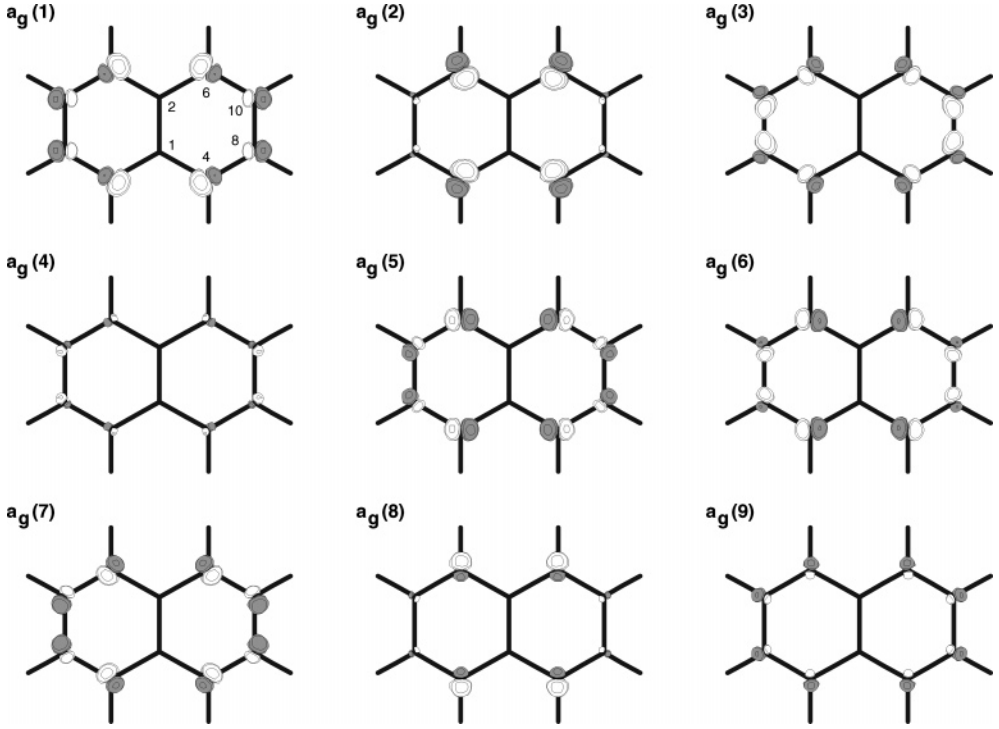

Figure 4. Top view of the vibronic coupling density using $\Delta\rho = \rho_F - \rho_0 = \rho_{LUMO}$ as the electron density difference. The white region is positive, and the gray region negative. The threshold of the isosurface is 5×10^{-5} atomic unit.

η on the C atoms are not symmetric. Thus the large net contribution to the vibronic coupling remains after cancellation.

Finally, the coupling of $a_g(7)$ looks large at a glance. However, the large density is canceled, and small coupling results.

5.2.5. Relaxed Vibronic Coupling Density. Figures 6 and 7 show the relaxed vibronic coupling density. Though it is more complex than that of the frozen density, reflecting the complicated distribution of the relaxed electron density, in principle, the distribution of Figures 6 and 7 can be understood from Figures 2b and 3.

As shown in Figures 6 and 7, both the π and σ electron density distributions contribute to the relaxed vibronic coupling density. The in-plane, or σ density also contributes to the coupling. To clarify this, the vibronic coupling density is integrated over the region of the Wigner−Seitz cell around a nucleus. The regional or atomic vibronic coupling constants are shown in Figures 8 and 9 for ρ_F and ρ_R, respectively. As a rule, the absolute values of the atomic vibronic coupling constant calculated from ρ_R become smaller than those from ρ_F. This is because of the polarization of the occupied electron density.

6. Nuclear Fukui Function

In this section, we discuss the relation between the vibronic coupling density and nuclear Fukui function,[33] which is based on the density functional theory.[40]

Assuming the BO approximation, from the Hohenberg−Kohn theorem, the ground state energy of a system is written as a functional of the ground state electron density ρ and potential u:

$$E[\rho,u] = T[\rho] + V_{ne}[\rho,u] + V_{ee}[\rho] + V_{nn}[u] = F[\rho] + U[\rho,u] \quad (21)$$

where $F[\rho] = T[\rho] + V_{ee}[\rho]$ and $U[\rho,u] = V_{ne}[\rho,u] + V_{nn}[u]$.

The total differential of $E[\rho,u]$ is
Because the electronic chemical potential is defined by

$$\mu = \mu[\rho,u] = \left(\frac{\partial E}{\partial N}\right)_u \quad (23)$$

and only $U[\rho,u]$ depends on u in $E[\rho,u]$,

$$dE = \mu\, dN + \int \left[\frac{\delta U}{\delta u}\right]_N \delta u(\mathbf{x})\, d\tau \quad (24)$$

The second term can be written in terms of normal coordinates:

$$dE = \mu\, dN + \sum_i \left(\frac{\partial U}{\partial Q_i}\right)_N dQ_i \quad (25)$$

Assuming the Hellmann−Feynman theorem,

$$\left(\frac{\partial U}{\partial Q_i}\right) = \int \rho_N(\mathbf{x})\, v_i(\mathbf{x})\, d\tau + \left(\frac{\partial V_{nn}}{\partial Q_i}\right) = V_i \quad (26)$$

From the mixed derivative of E with respect to N and Q_i, we obtain the Maxwell relation:

$$\left(\frac{\partial^2 E}{\partial N \partial Q_i}\right) = \left(\frac{\partial \mu}{\partial Q_i}\right)_N = \left[\frac{\partial}{\partial N}\left(\frac{\partial U}{\partial Q_i}\right)\right]_{Q_i} \quad (27)$$

The right-hand side is approximately equal to the finite difference

$$\left(\frac{\partial V_i}{\partial N}\right)_{Q_i} = \left[\frac{\partial}{\partial N}\left(\frac{\partial E}{\partial Q_i}\right)\right] \approx \left(\frac{\partial E_{N+1}}{\partial Q_i}\right) - \left(\frac{\partial E_N}{\partial Q_i}\right) \quad (28)$$

From eqs 8, 10, and 14,

$$\left(\frac{\partial \mu}{\partial Q_i}\right)_N = \left(\frac{\partial V_i}{\partial N}\right)_{Q_i} \approx \int \eta_i(\mathbf{x})\, d\tau = V_i \quad (29)$$

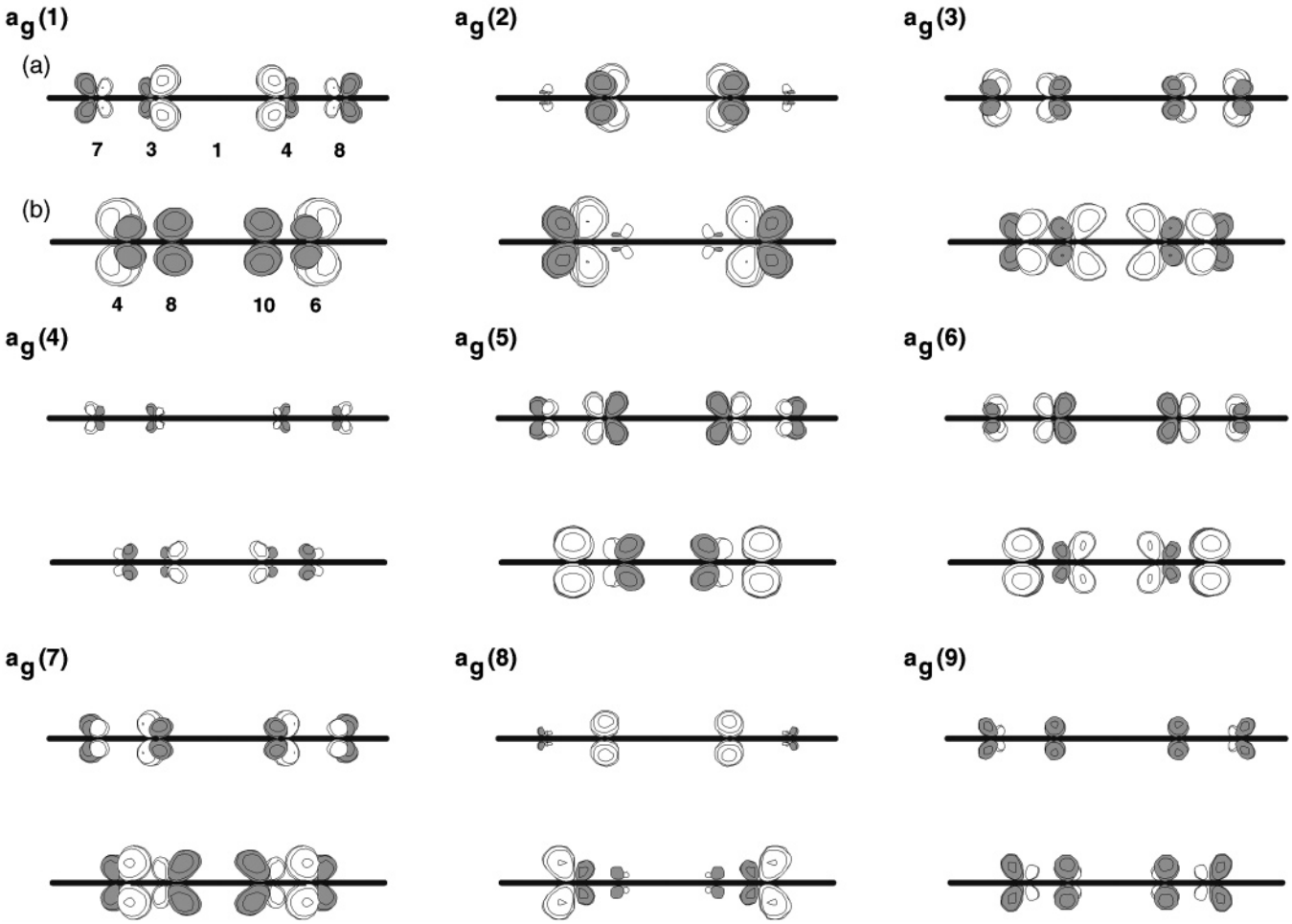

Figure 5. Side view of the vibronic coupling density using $\Delta\rho = \rho_F - \rho_0 = \rho_{LUMO}$ as the electron density difference. The white region is positive, and the gray region negative. The threshold of the isosurface is 5×10^{-5} atomic unit.

Furthermore, the total differential of the chemical potential $\mu = \mu[\rho,u]$ can be written as

$$d\mu = 2\eta\, dN + \sum_i \left(\frac{\partial \mu}{\partial Q_i}\right)_N dQ_i \tag{30}$$

where $\eta = {}^1/_2(\partial\mu/\partial N)_u$ is the absolute hardness. Therefore

$$d\mu = 2\eta\, dN + \sum_i V_i\, dQ_i = 2\eta\, dN + \sum_i \left(\int d\tau \eta_i(\mathbf{x})\right) dQ_i \tag{31}$$

On the other hand, the nuclear Fukui function is defined by

$$\phi_{k\alpha} = -\left(\frac{\partial U}{\partial x_{k\alpha}}\right)_N \tag{32}$$

where $x_{k\alpha}$ is the $k = x, y, z$ component of the position vector of a nucleus α. The total differential of the electronic chemical potential is written as

$$d\mu = 2\eta\, dN - \sum_\alpha \sum_{k=x,y,z} \phi_{k\alpha}\, dx_{k\alpha} \tag{33}$$

Moreover, the coordinates $x_{k\alpha}$ is related to the normal coordinate

$$Q_i = \sum_{k,\alpha} A_{i,k\alpha} x_{k\alpha} \tag{34}$$

and

$$d\mu = 2\eta\, dN + \sum_{k,\alpha} \sum_i \left(\int d\tau\, \eta_i(\mathbf{x})\right) A_{i,k\alpha}\, dx_{k\alpha} \tag{35}$$

Therefore, the nuclear Fukui function is expressed by the vibronic coupling constant, or vibronic coupling density

$$\phi_{k\alpha} = -\sum_i \left(\int d\tau\, \eta_i(\mathbf{x})\right) A_{i,k\alpha} = -\sum_i V_i A_{i,k\alpha} \tag{36}$$

From eq 29, the vibronic coupling constant means the sensitivity of the electronic chemical potential for the deformation Q_i, and the nuclear Fukui function describes that for the displacement $x_{k\alpha}$. The nuclear Fukui function is expressed as an element of a $3M$-dimensional vector, where M denotes the number of nuclei. On the other hand, the vibronic coupling density as a function of the position for a certain deformation. The vibronic coupling density has advantages in the following points. First, vibronic coupling density η yields the vibronic coupling constant and, thus, the nuclear Fukui function ϕ as described in eq 36. The vibronic coupling constant for a certain mode can be observed by spectroscopy. Therefore, one can compare the calculated vibronic coupling density with experiments. Second, contrast to the nuclear Fukui function, the vibronic coupling density is a local function of the position in a molecule. The vibronic

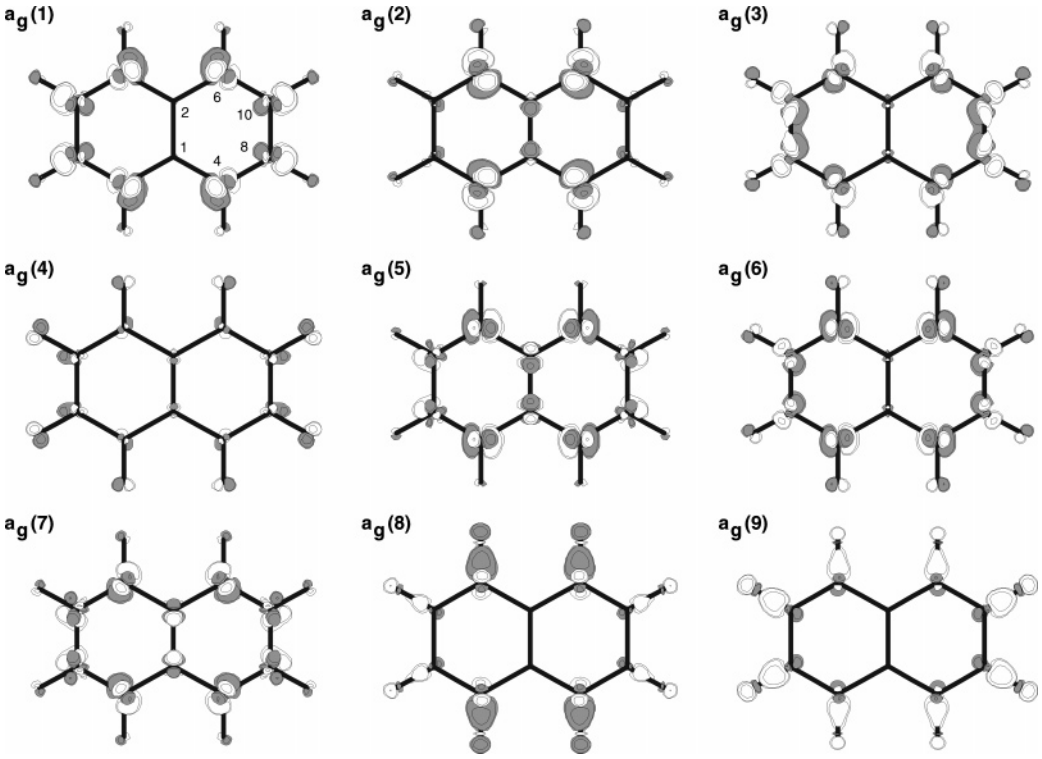

Figure 6. Top view of the vibronic coupling density using $\Delta\rho = \rho_R - \rho_0$ as the electron density difference. The white region is positive, and the gray region negative. The threshold of the isosurface is 5×10^{-5} atomic unit.

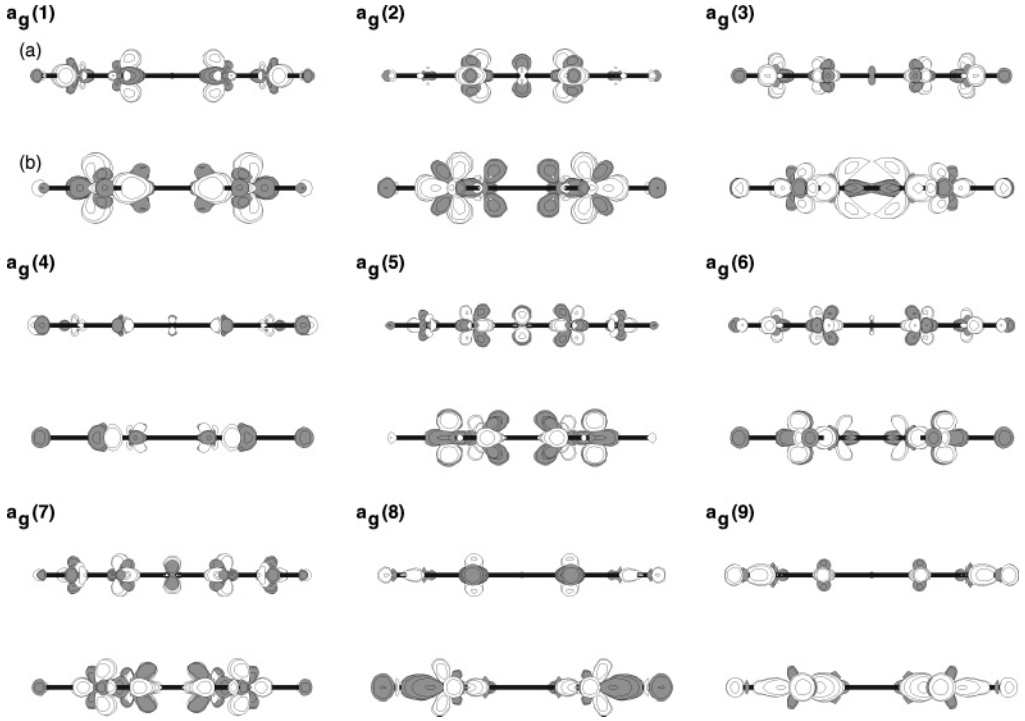

Figure 7. Side view of the vibronic coupling density using $\Delta\rho = \rho_R - \rho_0$ as the electron density difference. The white region is positive, and the gray region negative. The threshold of the isosurface is 5×10^{-5} atomic unit.

coupling is a driving force for the structural change in the early stage of a chemical reaction. From the vibronic coupling density map, one can see the region from which the large vibronic coupling comes. Therefore, for chemical reactions including solid-state reactions,[41] more detailed discussion on an active cite would be possible using the vibronic coupling density.

7. Conclusions

A method of vibronic coupling density analysis was extended for totally symmetric vibrational modes of a molecule including non-Jahn−Teller molecules. The method was applied for naphthalene anion to compare with benzene anion.

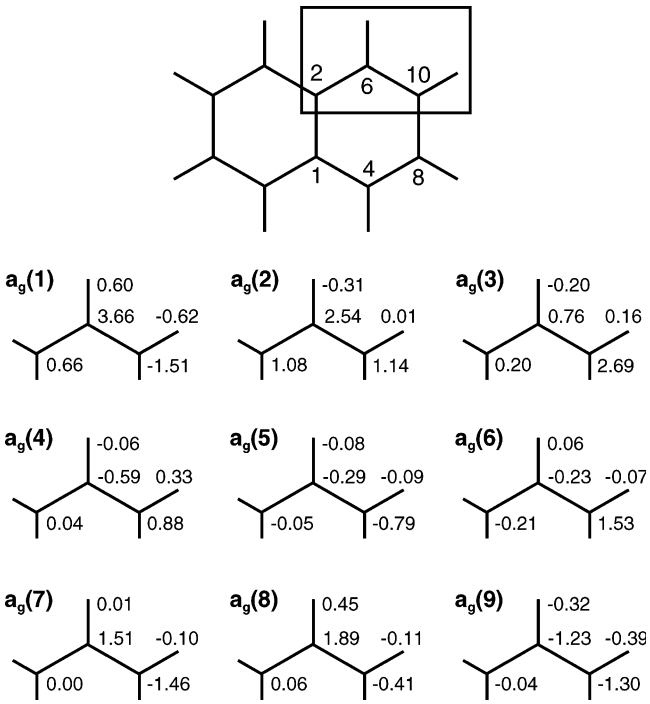

Figure 8. Regional vibronic coupling density (10^{-4} au), which is obtained by integration of the vibronic coupling density over the Wigner−Seits cell of each nucleus. The electron density difference employed is $\rho_F - \rho_0 = \rho_{LUMO}$.

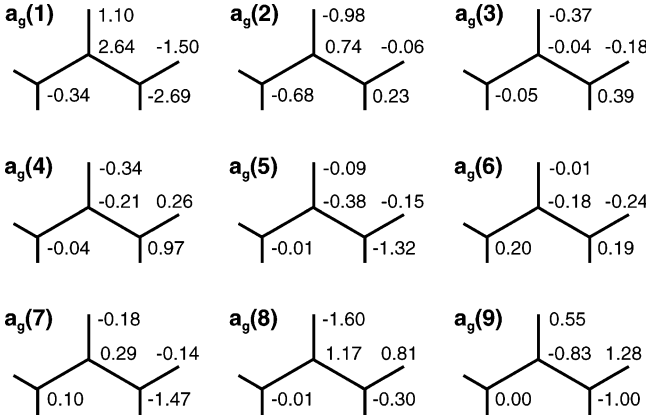

Figure 9. Regional vibronic coupling density (10^{-4} au), which is obtained by integration of the vibronic coupling density over the Wigner−Seits cell of each nucleus. The electron density difference employed is $\rho_R - \rho_0$.

$$dE = \left(\frac{\partial E}{\partial N}\right)_u dN + \int \left[\frac{\partial E}{\partial u}\right]_N \delta u(\mathbf{x})\, d\tau \qquad (22)$$

First, we calculated vibronic coupling constants using frozen electron density ρ_F, and the calculated values were overestimated. On the other hand, the relaxed electron density ρ_R gives a good result. Thus, it was found that, contrary to the non-totally-symmetric modes, the orbital relaxation upon the charge transfer plays a crucial role in the vibronic coupling calculation for non-Jahn−Teller molecule. This is because all the occupied orbitals contribute to the vibronic coupling.

Next, the relationship between the vibronic coupling density and the nuclear Fukui function was discussed. Vibronic coupling density is defined as a local function of the position, but the nuclear Fukui function is an element of a vector. The concept of vibronic coupling density has advantages in the discussion of chemical reactions. Applications of the vibronic coupling density analysis to chemical reactions including solid-state reactions, in which nuclear displacement plays an important role, are under investigation. They will be published elsewhere in the near future.

Acknowledgment. Numerical calculation was partly performed in the Supercomputer Laboratory of Kyoto University and Research Center for Computational Science, Okazaki, Japan.

References and Notes

(1) Fischer, G. *Vibronic Coupling*; Academic Press: London, 1984.
(2) Bersuker, I. B.; Polinger, V. Z. *Vibronic Interactions in Molecules and Crystals*; Springer: New York, 1989.
(3) Bersuker, I. B. *The Jahn-Teller Effect*; Cambdige University Press: Cambridge, U.K., 2006.
(4) Sato, T.; Tokunaga, K.; Tanaka, K. *J. Chem. Phys.* **2006**, *124*, 024314.
(5) Tokunaga, K.; Sato, T.; Tanaka, K. *J. Chem. Phys.* **2006**, *124*, 154303.
(6) Koch, E. E.; Otto, A.; Radler, K. *Chem. Phys. Lett.* **1972**, *16*, 131.
(7) Mikami, N.; Ito, M. *Chem. Phys. Lett.* **1975**, *31*, 472.
(8) Stockburger, M.; Gattermann, H.; Klusmann, W. *J. Chem. Phys.* **1975**, *63*, 4519.
(9) Stockburger, M.; Gattermann, H.; Klusman, W. *J. Chem. Phys.* **1975**, *63*, 4529.
(10) Mikami, N.; Ito, M. *Chem. Phys.* **1977**, *23*, 141.
(11) Beck, S. M.; Powers, D. E.; Hopkins, J. B.; Smalley, R. E. *J. Chem. Phys.* **1980**, *73*, 2019.
(12) Beck, S. M.; Hopkins, J. B.; Powers, D. E.; Smalley, R. E. *J. Chem. Phys.* **1981**, *74*, 43.
(13) Behlen, F. M.; McDonald, D. B.; Sethuraman, V.; Rice, S. A. *J. Chem. Phys.* **1981**, *75*, 5685.
(14) Duncan, M. A.; Dietz, T. G.; Smalley, R. E. *J. Chem. Phys.* **1981**, *75*, 2118.
(15) Salama, F.; Allamandola, J. *J. Chem. Phys.* **1991**, *94*, 6964.
(16) Cockett, M. C. R.; Ozeki, H.; Okuyama, K.; Kimura, K. *J. Chem. Phys.* **1993**, *98*, 7763.
(17) Negri, F.; Zgierski, M. Z. *J. Chem. Phys.* **1996**, *104*, 3486.
(18) Negri, F.; Zgierski, M. Z. *J. Chem. Phys.* **1997**, *107*, 4827.
(19) Brundle, C. R.; Robin, M. B.; Kuebler, N. A. *J. Am. Chem. Soc.* **1972**, *94*, 1466.
(20) Andrews, L.; Blankenship, T. A. *J. Am. Chem. Soc.* **1981**, *103*, 5977.
(21) Andrews, L.; Kelsall, B. J.; Blankenship, T. A. *J. Phys. Chem.* **1982**, *86*, 2916.
(22) Hacaloglu, J.; Andrews, L. *Chem. Phys. Lett.* **1989**, *160*, 274.
(23) Rühl, E.; Price, S. D.; Leach, S. *J. Phys. Chem.* **1989**, *93*, 6312.
(24) Szczepanski, J.; Roser, D.; Personette, W.; Eyring, M.; Pellow, R.; Vala, M. *J. Phys. Chem.* **1992**, *96*, 7876.
(25) Negri, F.; Zgierski, M. Z. *J. Chem. Phys.* **1993**, *100*, 1387.
(26) da Silva Filho, D. A.; Friedlein, R.; Coropceanu, V.; Öhrwall, G.; Osikowicz, W.; Suess, C.; Sorensen, S. L.; Svensson, S.; Salaneck, W. R.; Brédas, J. L. *Chem. Commun.* **2004**, page 1702.
(27) Schiedt, J.; Knott, W. J.; Barbu, K. L.; Schlag, E. W.; Weinkauf, R. *J. Chem. Phys.* **2000**, *113*, 9470.
(28) Lyapustina, S. A.; Xu, S.; Nilles, J. M.; Bowen, K. H. J. *J. Chem. Phys.* **2000**, *112*, 6643.
(29) Song, J. K.; Han, S. Y.; Chu, I.; Kim, J. H.; Kim, S. K.; Lyapustina, S. A.; Xu, S.; Nilles, J. M.; Bowen, K. H. J. *J. Chem. Phys.* **2002**, *116*, 4477.
(30) Devos, A.; Lannoo, M. *Phys. Rev. B* **1997**, *58*, 8236.
(31) Kato, T.; Yamabe, T. *J. Chem. Phys.* **2001**, *115*, 8592.
(32) Klimkāns, A.; Larsson, S. *Chem. Phys.* **1994**, *189*, 25.
(33) Cohen, M. H.; Ganduglia-Pirovano, M. V.; Kudrnovský, J. *J. Chem. Phys.* **1994**, *101*, 8988.
(34) Non-zero cross terms are due to the Duschinsky effect. We calculated Duschinsky matrix **S**, $\mathbf{Q}' = \mathbf{SQ}$, where $\mathbf{Q}'$ and **Q** are the normal modes of the naphthalene and the naphthalene anion. The smallest diagonal terms of *S* are 0.92−0.93 for $a_g(6)$ and $a_g(7)$, which is larger than that of benzene. In other words, the Duschinsky effect of naphthalene is less important than that for benzene. Moreover, the off-diagonal elements other than that between $a_g(6)$ and $a_g(7)$ are small, and the diagonal elements are almost equal to unity. Therefore, the Duschinsky effect does not play an important role in the present system, and we neglect the cross term in the fourth term of eq 4.
(35) Feynman, R. P. *Phys. Rev.* **1939**, *56*, 340.
(36) Nakatsuji, H.; Kanda, K.; Yonezawa, T. *Chem. Phys. Lett.* **1980**, *75*, 340−346.
(37) Schmidt, M. W.; Baldridge, K. K.; Boatz, J. A.; Elbert, S. T.; Gordon, M. S.; Jensen, J. H.; Koseki, S.; Matsunaga, N.; Nguyen, K. A.;

Su, S. J.; Windus, T. L.; Dupins, M.; Montgomery, J. A. *J. Comput. Chem.* **1993**, *14*, 1347.

(38) Hanson, D. M.; Gee, A. R. *J. Chem. Phys.* **1969**, *51*, 5052.

(39) Frisch, M. J.; Trucks, G. W.; Schlegel, H. B.; Scuseria, G. E.; Robb, M. A.; Cheeseman, J. R.; Montgomery, J. A., Jr.; Vreven, T.; Kudin, K. N.; Burant, J. C.; Millam, J. M.; Iyengar, S. S.; Tomasi, J.; Barone, V.; Mennucci, B.; Cossi, M.; Scalmani, G.; Rega, N.; Petersson, G. A.; Nakatsuji, H.; Hada, M.; Ehara, M.; Toyota, K.; Fukuda, R.; Hasegawa, J.; Ishida, M.; Nakajima, T.; Honda, Y.; Kitao, O.; Nakai, H.; Klene, M.; Li, X.; Knox, J. E.; Hratchian, H. P.; Cross, J. B.; Adamo, C.; Jaramillo, J.; Gomperts, R.; Stratmann, R. E.; Yazyev, O.; Austin, A. J.; Cammi, R.; Pomelli, C.; Ochterski, J. W.; Ayala, P. Y.; Morokuma, K.; Voth, G. A.; Salvador, P.; Dannenberg, J. J.; Zakrzewski, V. G.; Dapprich, S.; Daniels, A. D.; Strain, M. C.; Farkas, O.; Malick, D. K.; Rabuck, A. D.; Raghavachari, K.; Foresman, J. B.; Ortiz, J. V.; Cui, Q.; Baboul, A. G.; Clifford, S.; Cioslowski, J.; Stefanov, B. B.; Liu, G.; Liashenko, A.; Piskorz, P.; Komaromi, I.; Martin, R. L.; Fox, D. J.; Keith, T.; Al-Laham, M. A.; Peng, C. Y.; Nanayakkara, A.; Challacombe, M.; Gill, P. M. W.; Johnson, B.; Chen, W.; Wong, M. W.; Gonzalez, C.; Pople, J. A. *Gaussian 03*, revision C.02; Wallingford CT, 2004.

(40) Parr, R. G.; Yang, W. *Density-Functional Theory of Atoms and Molecules*; Oxford University Press: New York, 1989.

(41) Feng, S.; Li, T. *J. Phys. Chem. A* **2005**, *109*, 7258.

(42) Scott, A. P.; Radom, L. *J. Phys. Chem.* **1996**, *100*, 16502.